The influence of slightly and highly soluble carbonate salts on phase relations in hydrated calcium aluminate cements

Guillermo Puerta-Falla, Magdalena Balonis, Gwenn Le Saout, Aditya Kumar, Melanie Rivera, Gabriel Falzone, Narayanan Neithalath, Gaurav Sant

The influence of slightly and highly soluble carbonate salts on phase relations in hydrated calcium aluminate cements

Guillermo Puerta-Falla[1], Magdalena Balonis[2,3], Gwenn Le Saout[4], Aditya Kumar[1],
Melanie Rivera[1], Gabriel Falzone[1], Narayanan Neithalath[5], and Gaurav Sant[1,6,*]

[1] Laboratory for the Chemistry of Construction Materials, Department of Civil and Environmental Engineering, University of California, Los Angeles, CA, USA

[2] Department of Materials Science and Engineering, University of California, Los Angeles, CA, USA

[3] Institute for Technology Advancement, University of California, Los Angeles, CA, USA

[4] Centre des Matériaux de l'École des Mines d'Alès (C2MA), École des mines d'Alès, Alès, France

[5] School of Sustainable Engineering and the Built Environment (SSBE), Arizona State University, Tempe, AZ, USA

[6] California Nanosystems Institute (CNSI), University of California, Los Angeles, CA, USA

ABSTRACT

The addition of slightly ($CaCO_3$) and highly soluble (Na_2CO_3) carbonate salts is expected to favor the formation of carboaluminate phases in hydrated calcium aluminate cements (CACs). A multi-method approach including X-ray diffraction, thermogravimetric analysis, and thermodynamic calculations is applied to highlight that the "conversion phenomena" in CACs cannot be mitigated by the formation of carboaluminate phases (monocarboaluminate: Mc and hemicarboaluminate: Hc) which are anticipated to form following the addition of carbonate salts. Here, carboaluminate phase formation is shown to depend on three factors: (1) water availability, (2) carbonate content of the salts, and their ability to mobilize CO_3^{2-} species in solution, and (3) lime content associated with the carbonate salt. The latter two factors are linked to the composition and solubility of the carbonate agent. It is concluded that limestone ($CaCO_3$), despite being a source of calcium and carbonate species, contributes only slightly to carboaluminate phase formation due to its low solubility and slow dissolution rate. Soluble carbonate salts (Na_2CO_3) fail to boost carboaluminate phase formation as the availability of Ca^{2+} ions and water are limiting. Detailed thermodynamic calculations are used to elucidate conditions that affect the formation of carboaluminate phases.
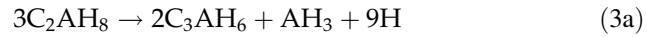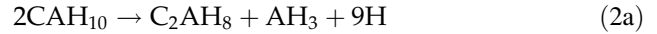
Introduction

In recent years, the use of powdered limestone (calcite) has emerged as a route to reduce the ordinary portland cement (OPC) content of the binder phase in concrete. The kinetic and thermodynamic implications of limestone addition to OPC have been widely studied in terms of the filler effects of limestone and stabilization of ettringite (AFt) which prevents its conversion to monosulfoaluminate (SO_4-AFm, Ms). [1–12]. But studies describing the effects of limestone additions to calcium aluminate cements (CACs) are less common, likely on account of complexities in reactions in CACs, e.g., involving phase conversions, temperature dependence of phase equilibria, and the specialty use of CACs, as a result of which such cements account for only a small fraction of the total cement use [13–17].
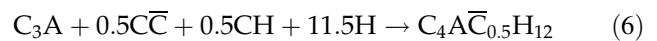
The primary reactive compounds in CACs include monocalcium aluminate $CaO \cdot Al_2O_3$ (CA) and gehlenite $2CaO \cdot SiO_2 \cdot Al_2O_3$ (C_2AS)[1]. Since C_2AS is slightly reactive at ambient temperatures, most studies simplify the hydration of CACs as the reaction of CA with water [18]. In water-rich systems (i.e., when $w/c > 0.50$, w/c: water-to-cement ratio, by mass) at ambient temperatures ($T < 30$ °C), CACs hydrate to form CAH_{10}, C_2AH_8, and AH_3 as the initial ("early") hydration products (Eqs. 1–3a, 3b). The two former hydrates are termed as *metastable*, as in time they transform to C_3AH_6 which coexists with AH_3, and stratlingite phases at "mature" times [19]. Since this nature of phase transformations involves the expulsion of water from the solids, the resulting accumulation of water in the microstructure results in an increase in porosity, and a detrimental reduction in the mechanical properties [20–22]. This process is termed as "conversion" [16].

Recently, Falzone et al. [13] showed that the reaction pathway involving the formation of the metastable hydrates (i.e., CAH_{10}, C_2AH_8) and their conversion to C_3AH_6 can be bypassed by the addition of calcium nitrate ($Ca(NO_3)_2$). This is due to the formation of the NO_3-AFm phase, which acts to circumvent/bypass the conversion process.

---

[1] Standard cement chemistry notation is used. As per this simplified notation: C = CaO, A = Al_2O_3, F = Fe_2O_3, S = SiO_2, CS = $CaSO_4 \cdot 2H_2O$, H = H_2O, and $\overline{C}$ = CO_2.

$$CA + 10H \rightarrow CAH_{10} \tag{1}$$

$$2CAH_{10} \rightarrow C_2AH_8 + AH_3 + 9H \tag{2a}$$

$$2CA + 11H \rightarrow C_2AH_8 + AH_3 \tag{2b}$$

$$3C_2AH_8 \rightarrow 2C_3AH_6 + AH_3 + 9H \tag{3a}$$

$$3CA + 12H \rightarrow C_3AH_6 + 2AH_3 \tag{3b}$$

It is postulated that similar to calcium nitrate, limestone and sodium carbonate, due to their ability to provision CO_3^{2-} ions and the potential to stabilize the CO_3-AFm compounds (i.e., monocarboaluminate, Mc, and hemicarboaluminate, Hc, as shown in Eqs. 4–6), should also be able to prevent conversion [8, 23]. Based on this concept, Luz and Pandolfelli [24] showed that the addition of $CaCO_3$ to CACs does result in the formation of the carboaluminate phases which can somewhat inhibit phase conversion. However, recent studies have shown that the reaction of limestone with CACs is kinetically hindered in spite of being thermodynamically favored [12]. It is therefore postulated that for carboaluminate phase formation to be enhanced, a carbonate source with high solubility, and fast dissolution, i.e., a soluble carbonate salt similar to $Ca(NO_3)_2$, needs to be provisioned. Based on this idea, this study examines the influences of two carbonate salts of low (limestone, $CaCO_3$) and high solubility (sodium carbonate, Na_2CO_3) on hydrated phase relations in CACs. The role of water availability is discussed in terms of impacts on carboaluminate phase formation. Special focus is paid to understand if the supply of a suitable carbonate source can indeed suppress phase conversion reactions in calcium aluminate cements.

$$3CA + C\overline{C} + 17H \rightarrow C_4A\overline{C}H_{11} + 2AH_3 \tag{4}$$

$$C_3AH_6 + C\overline{C} + 5H \leftrightarrow C_4A\overline{C}H_{11} \tag{5}$$

$$C_3A + 0.5C\overline{C} + 0.5CH + 11.5H \rightarrow C_4A\overline{C}_{0.5}H_{12} \tag{6}$$

Materials and methods

A commercially available grey calcium aluminate cement (CAC) Secar 51 that is produced by Kerneos Aluminate Technologies was used. The oxide composition of the CAC as determined by X-ray fluorescence (XRF) in mass% was as follows: 4.9 % SiO_2, 52.1 % Al_2O_3, 2.3 % Fe_2O_3, 39.8 % CaO, 0.60 % MgO, 0.07 % Na_2O, and 0.31 % K_2O. The mineralogical (phase) composition of the CAC as determined from

Rietveld analysis of its X-ray diffraction patterns in mass% was as follows: 73.3 % CA, 18.1 % C_2AS, 4.9 % CT, 1.5 % C_3FT, 0.6 % C_2F, 0.8 % CaO, and 0.8 % Fe_2O_3. A nominally pure limestone powder (>95 % $CaCO_3$) was sourced from OMYA A.G.[2] Analytical reagent-grade sodium carbonate was purchased from Sigma-Aldrich (CAS Number: 497-19-8).

A series of cementitious mixtures (Table 1) were prepared using de-ionized (DI) water at 3 different water-to-solid ratios (w/s = 0.40, 0.45, and 0.70, by mass) as described in ASTM C305 [25]. In samples where CAC was replaced by limestone, the CAC and limestone were "dry mixed" prior to the addition of water. For blends where CAC was replaced by sodium carbonate, sodium carbonate was dissolved in water, and the CAC was then mixed into this solution. It should be noted that the w/s listed corresponds to the water-to-solid (i.e., CAC, sodium carbonate and limestone) ratio on a mass basis. The replacement of CAC by a carbonate source alters the (a) equivalent carbon dioxide-to-aluminum oxide ($CO_{2\text{-eq}}/Al_2O_3$) ratio, (b) calcium-to-aluminum oxide (CaO/Al_2O_3) ratio, and (c) equivalent carbon dioxide-to-calcium oxide ($CO_{2\text{-eq}}/CaO$) ratio (all on a mass basis). Trends in these ratios as a function of CAC replacement level are shown in Fig. 1.

The particle size distributions (PSDs, Fig. 1d) of all the solids were measured using a Beckman Coulter Static Light Scattering Analyzer (LS13-320). Powders were dispersed to their primary particles by sonication in isopropanol. The uncertainty in the light scattering analysis was around 6 % based on six replicates and assuming the refractive index of the CAC, limestone, and anhydrous Na_2CO_3 to be 1.7, 1.69, and 1.535, respectively [26].

The compressive strength of the w/s = 0.45 mixtures (see Table 1) was measured at 1, 3, 7, 28, and 90 days using cubic specimens (50 × 50 × 50 mm) cured at 25 ± 1 °C in lime water as described in ASTM C109 [25]. The strength reported is the average of three specimens cast from the same mixing batch.

Table 1 An overview of the cementitious formulations used in this study

Mixture ID	w/s	Replacement by $CaCO_3$ (%)	Replacement by Na_2CO_3 (%)
SEC	0.45	0	0
10LSEC	0.40, 0.45, 0.70	10	0
30LSEC	0.45	30	0
50LSEC	0.45	50	0
10NSEC	0.40, 0.70	0	10
30NSEC	0.70	0	30

X-ray diffraction (XRD) patterns were obtained on finely powdered samples at desired ages using a Bruker D8 Advance diffractometer in a θ–θ configuration using Cu-Kα radiation (λ = 1.54 Å). The samples were scanned between 5° and 70° (2θ, degrees) in continuous mode with an integrated step scan of 0.017° (2θ, degrees) using a VANTEC detector. The total time required for acquisition of the X-ray diffraction pattern was around 12 min. A fixed divergence slit of 0.50° was used during data acquisition. Care was taken to minimize preferred orientation errors by texturing the surfaces of the sample. Information on the X-ray structures of anhydrous and hydrated crystalline phases was sourced from standard databases (ICDD [27]) or the literature [28]. The anhydrous CAC was analyzed using a protocol described by Le Saout et al. [29].

A Perkin Elmer STA 6000 simultaneous thermal analyzer (TGA/DTG/DTA) equipped with a Pyris data acquisition interface was used to identify and quantify solid phases present in the cementitious mixtures. The temperature and mass sensitivity of this instrument are ±0.25 °C and ±0.1 μg, respectively. To arrest hydration, solvent exchange was performed using isopropanol wherein at a desired age, hydrated pastes were crushed to a size less than 5 mm and submerged in isopropanol for 14 days, with isopropanol being replaced every 7 days. Following such solvent exchange, samples were placed under vacuum in a desiccator to remove the solvent for another 7 days. During measurement, powder samples were placed in pure aluminum oxide crucibles under the UHP-N_2 purge at a flow rate of 20 ml/min and heated at a rate of 10 °C per minute over a temperature range from 35 to 975 °C. The weight loss (TG) and differential weight loss (DTG) patterns acquired were used to quantify the amount of $CaCO_3$ present in the system. It should be noted
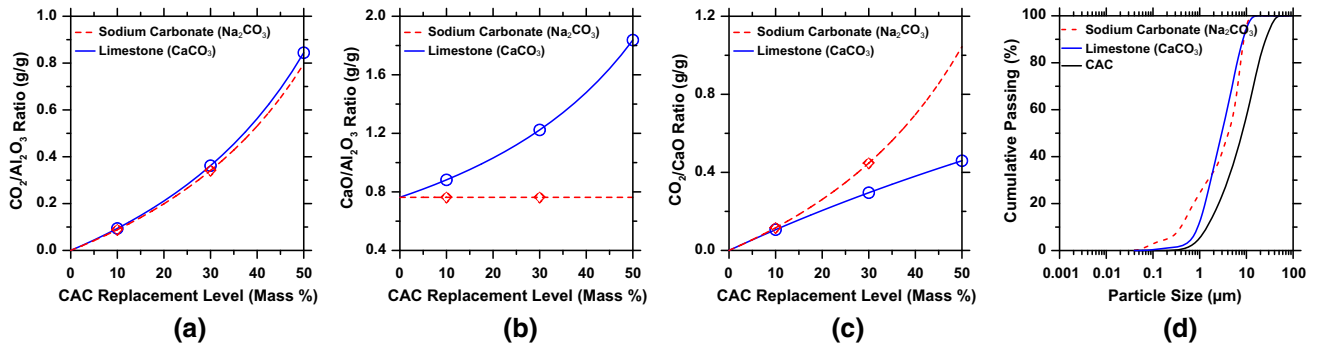
Figure 1 **a** Carbon dioxide equivalent-to-aluminum oxide ($CO_{2\text{-eq}}/Al_2O_3$), **b** calcium-to-aluminum oxide (CaO/Al_2O_3), and **c** carbon dioxide equivalent-to-calcium oxide ($CO_{2\text{-eq}}/CaO$) mass ratios as a function of the CAC replacement level for each carbonate source. **d** Particle size distributions (PSDs) of the solid reactants used in this study.

that the quantity of $CaCO_3$ is presented as a percentage of the phase present per dry mass of paste (% dry mass).

Thermodynamic calculations

Thermodynamic calculations were carried out using a geochemical speciation program, GEMS-PSI, Gibbs Energy Minimization Software, ver. 2.3 [30]. GEMS-PSI uses the initial mixture proportions represented in the form of the simple oxides present in the solid precursors and the water content, as inputs, and applies a convex programming approach in conjunction with data of the thermodynamic properties of phases (solids, liquid, and air) to compute equilibrium phase balances and ion speciation in a multicomponent system. The input oxide composition of the CAC was obtained from the XRF data. To simulate different levels of CAC reaction, the oxides present in the CAC were allowed to react in incremental steps of 10 %, from 0 to 100 % reaction with the total amount of water and carbonate source present. It should be noted that this approach does not consider the kinetics, i.e., the rate of reaction of the different phases in a CAC. Rather, it seeks to understand the evolution of phase balances with increasing reaction extent—assuming that in any given reaction step, the reactants are completely transformed to suitable products, to minimize the free energy. Thus, this "fractional reaction" approach elucidates the development of hydrated phases in the style of a step-wise reaction sequence [31–33].

Thermodynamic data of solid and aqueous species were sourced from the built-in GEMS-PSI (NAGRA) database of minerals, and amended with additional data relevant to cementitious systems as embedded in the CEMDATA07 database [14, 34–37]. The thermodynamic database was further expanded to consider gaylussite and thermonatrite as these phases were found to exist in Na_2CO_3-bearing blends [38] (see Table 2). Natron was also included to determine if this phase has a potential to form, and persists in blends containing higher Na_2CO_3 contents. The Gibbs free energy ($\Delta_f G^0$) of formation at $T = 25\ °C$ and $p = 1$ bar along with other thermodynamic properties (e.g., enthalpy and entropy of formation) and the molar volumes of these phases were adapted from the THERMODDEM database [38] (Table 2). All simulations are carried out at $p = 1$ bar and $T = 25\ °C$ in CO_2-free air. It is important to note that the simulations presented do not account for the influences of temperature change on phase relations, e.g., due the exothermic nature of CAC hydration. The simulations presented apply to two different scenarios: (i) "mature" time scales where C_3AH_6 and AH_3 are the stable hydrates that persist, and (ii) "early" times where the metastable hydrates such as CAH_{10}, C_2AH_8, and AH_3 persist, while the C_3AH_6 phase is suppressed from forming. For example, the mature age scenario is simulated by restricting the formation of the metastable hydrates and vice versa. For the sake of clarity, since the present work seeks to understand the influences of carbonate salts on preventing conversion (i.e., preventing the C_3AH_6 phase from forming at later times), only results corresponding to mature systems are presented.

Table 2 Thermodynamic data for relevant compounds at $T = 25\ °C$ and $p = 1$ bar which are used in calculations of phase equilibria

Phase	$\Delta_f G^0$ [kJ/mol]	$\Delta_f H^0$ [kJ/mol]	S^0 [J/K/mol]	a_0	a_1	a_2	a_3	V [cm^3/mol]
C_3AH_6	−5010.1	−5540	419	292	0.561			150
C_4AH_{13} (hydroxy-AFm)	−7326.6	−8302	700	711	1.047		−1600	274
C_4AcH_{11} monocarboaluminate	−7337.5	−8250	657	618	0.982	−2590000		261
$C_4Ac_{0.5}H_{12}$ hemicarboaluminate	−7336	−8270	713	664	1.014	−1300000	−800	285
C_2ASH_8 (strätlingite)	−5705.1	−6360	546	438	0.749	−1130000	−800	216
M_4AH_{10} (OH−hydrotalcite)	−6394.56	−7196	549	−364	4.21	3750000	629	220
M_4AcH_9 (CO$_3$-hydrotalcite)	−6580.15	−7374	551	−382	4.24	4320000	629	220
Brucite, $Mg(OH)_2$	−832.23	−923	63	101	0.017	−2560000		25
Water (H_2O)	−237.2	−286	70	75				18
SiO_2 (amorphous)	−848.9	−903	41	47	0.034	−1130000		29
$Fe(OH)_3$ (microcrystalline)	−711.6	−844	88	28	0.052			34
$Al(OH)_3$ (amorphous)	−1143.21	−1281	70	36	0.191			32
$Al(OH)_3$ (gibbsite)	−1151	−1289	70	36	0.191			32
Portlandite, $Ca(OH)_2$, CH	−897	−985	83	187	−0.02		−1600	33
Calcite, $CaCO_3$,CC	−1129.2	−1207	93	105	0.022	−2590000		37
Gypsum, $CaSO_4 \cdot 2H_2O$	−1797.8	−2023	194	91	0.318			75
Gaylussite, $Na_2Ca(CO_3)_2 \cdot 5H_2O$ [38]	−3372	−3834	387	[a]				148
Thermonatrite, $Na_2CO_3 \cdot H_2O$ [38]	−1286.2	−1430	168	149				54.8
Natron $Na_2CO_3 \cdot 10H_2O$ [38]	−3427.9	−4079	565	550				196

a_0, a_1, a_2, a_3 are empirical coefficients of the heat capacity equation: $C_p = a_0 + a_1T + a_2T^{-2} + a_3T^{-0.5}$; no value = 0.

[a] not available

Experimental results and discussion

Influence of limestone (slightly soluble carbonate) additions

Figure 2a shows compressive strength evolutions of mixtures prepared with various levels of CAC replaced by limestone. At any given age, the compressive strength reduces as the amount of limestone replacing CAC is increased. To account for dilution (i.e., reduction of the CAC content), the compressive strength at 90 days was plotted as a function of the CAC fraction in the pastes (Fig. 2b). Despite the reduction in strength with a decrease in the CAC
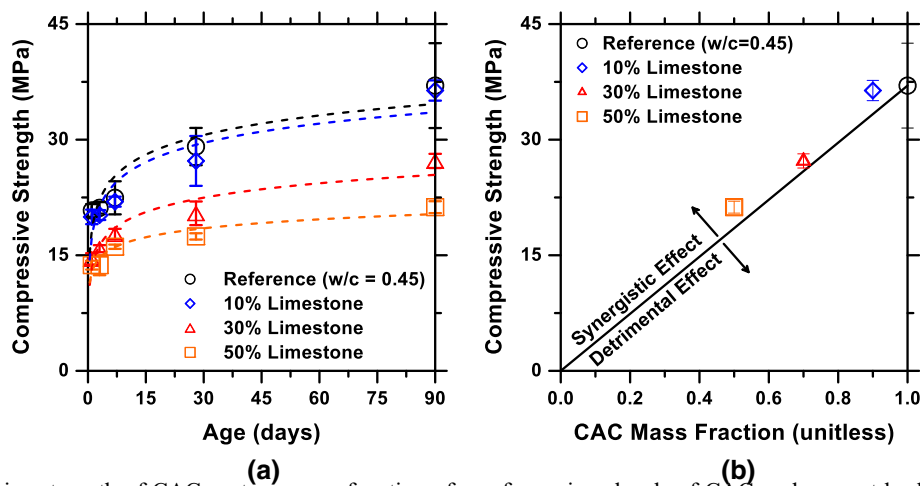

Figure 2 Compressive strength of CAC pastes: **a** as a function of age for various levels of CAC replacement by limestone and **b** after 90 days of hydration as a function of the CAC mass fraction in the binder. For all the mixtures illustrated in the figure, $w/s = 0.45$.

content, the strength values remain somewhat above the "dilution line." This implies that the inclusion of limestone results in synergistic effects—which, however, are not sufficient to prevent reductions in strength caused due to dilution. As noted in Fig. 2a, all mixtures show a steady increase in strength with age—at ambient curing temperatures (25 °C), a low temperature which is known to delay the onset of the conversion process [24, 39]. Furthermore, Scrivener et al. [16] noted that compressive strength development in large CAC samples (i.e., more than a few centimeters thick) is different from that in thinner samples, due to significant heat generation which results in accelerated conversion reactions in the former. After conversion has been completed, it is postulated that further strength gain may be associated with the formation of increasing quantities of C_3AH_6, Mc, or due to the hydration of residual unhydrated CAC [16] as water released from the metastable hydrates becomes available for reaction.

Figure 3 shows the development of phase assemblages, assessed by qualitative XRD, in blends where 10 % (by mass) of the CAC is replaced by limestone. It was observed that an increase in the water content (w/s) results in increased monocarboaluminate (Mc) formation (i.e., based on simple peak height comparisons), and the reduced formation of C_3AH_6—an outcome which may be associated with inhomogeneous water distributions in the microstructure. The enhanced formation of Mc occurs in conjunction with

the consumption of $CaCO_3$ (as also verified from TGA quantifications; Fig. 4), since the latter is a reactant in the formation of Mc. The consumption of $CaCO_3$ is accelerated by increasing water content as more limestone solubilizes increasing water availability. For example, after 90 days of hydration in a blend which initially contained 10 mass% limestone, there is less than 2 mass% unreacted limestone present in a system prepared at $w/s = 0.70$, while around 5 mass% limestone persists in a system prepared at
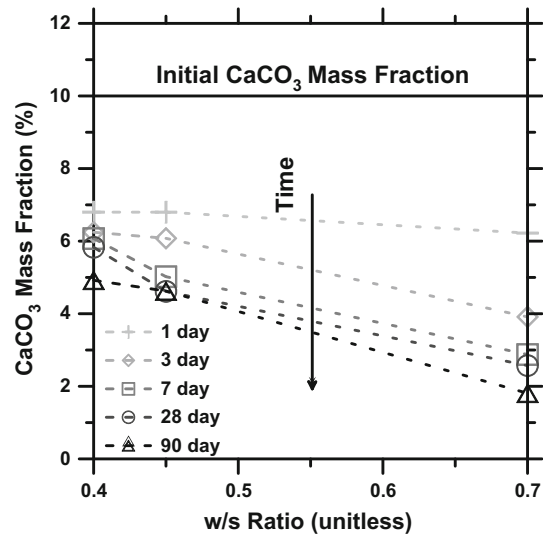
Figure 4 Residual $CaCO_3$ content quantified using thermal analysis (TGA/DTG) in CAC–limestone blends wherein 10 mass% of the CAC was replaced by limestone at different w/s.
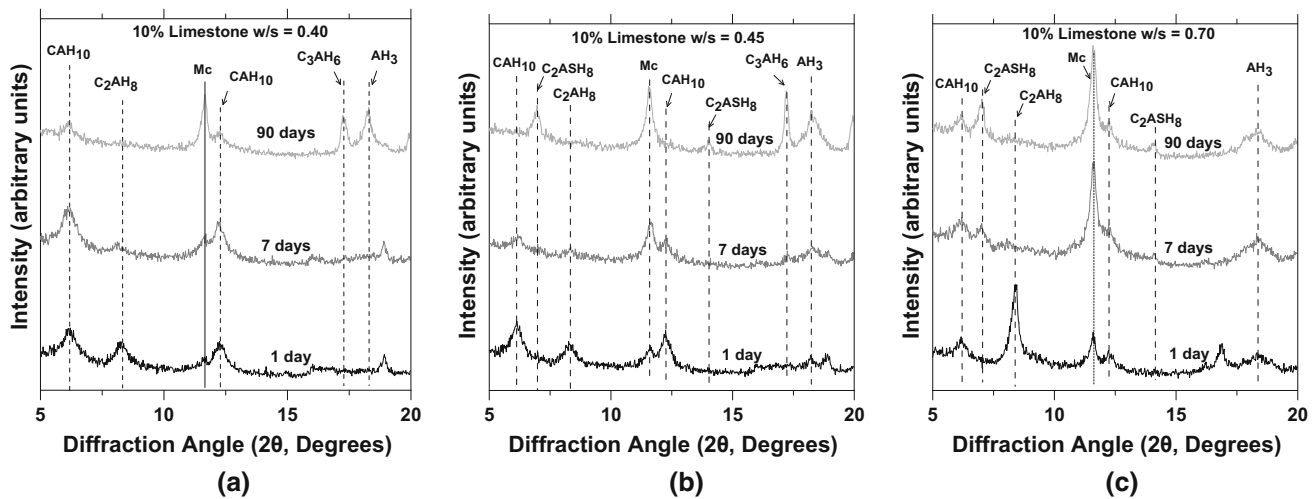
Figure 3 Representative XRD patterns for the hydrated blends wherein 10 mass% of CAC has been replaced by limestone for blends prepared at **a** $w/s = 0.40$, **b** $w/s = 0.45$, and **c** $w/s = 0.70$.
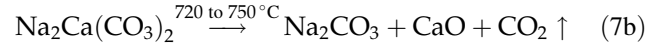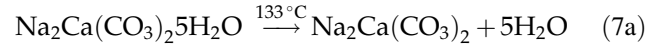
In all plots, *Mc* denotes the monocarboaluminate phase ($Ca_4Al_2(CO_3)(OH)_{12} \cdot 5H_2O$).

$w/s = 0.40$. The reduced quantity of C_3AH_6 which was noted with increasing w/s is likely on the account of a larger water content which favors the formation of CAH_{10} and C_2AH_8—whose formation is favored at the expense of C_3AH_6 at early ages. In fact, the formation of the C_2AH_8 phase serves as a transitory step in the formation of C_3AH_6 [13, 14].

The XRD patterns shown in Fig. 3 revealed Mc as the only carboaluminate phase (i.e., no Hc is detected) formed independent of w/s or age. This is likely on account of maintenance of a suitable $[CO_3^{2-}]/$ $[OH^-]$ molar ratio in solution which favors the formation of Mc, at the expense of Hc. This is a significant observation in comparison with OPC systems where Hc initially forms and over time transforms to Mc as calcite dissolution progresses [40]. The formation of strätlingite (C_2ASH_8) is favored with increasing water availability. The formation of strätlingite suggests the hydration of gehlenite (C_2AS), a low reactivity phase [15]. These results, therefore, indicate that the reactivities of both limestone and of C_2AS and hence the formation of Mc and C_2ASH_8 are enhanced in CAC blends with a higher water content and water activity [13].

Influence of sodium (highly soluble) carbonate additions

Figures 5–6 show representative XRD patterns and DTG curves of water-rich ($w/s = 0.70$) CAC blends prepared with sodium carbonate—where 10 and 30 mass% of the CAC have been replaced by Na_2CO_3. Several differences with respect to limestone systems were identified. First, it was noted that, unlike systems containing limestone, an increase in the amount of the carbonate source (Na_2CO_3) does not increase the amount of the carboaluminate phase formed. Instead, Na_2CO_3 appears to combine with Ca^{2+} ions present in the solution to form gaylussite ($Na_2Ca(CO_3)_2 \cdot 5H_2O$) and minor amounts of thermonatrite ($Na_2CO_3 \cdot H_2O$)—whose presence was verified by DTG analyses (Fig. 6), which shows characteristic dehydration and decarbonation peaks for the former at 133 °C and 720–750 °C, respectively (Eqs. 7a,7b [41]), and for the latter at around 100 °C [42, 43]. Since both gaylussite and thermonatrite are "water-rich phases" containing 5 and 1 formula units of water, respectively, the formation of these phases is suppressed in systems that are water deficient (e.g., $w/s = 0.40$; see Figs. 5a and 6a).

$$Na_2Ca(CO_3)_25H_2O \xrightarrow{133\,°C} Na_2Ca(CO_3)_2 + 5H_2O \quad (7a)$$

$$Na_2Ca(CO_3)_2 \xrightarrow{720 \text{ to } 750\,°C} Na_2CO_3 + CaO + CO_2 \uparrow \quad (7b)$$

Significantly, the conversion of metastable calcium aluminate hydrates (i.e., CAH_{10} and C_2AH_8) to C_3AH_6 occurs despite provision of a carbonate source and water (Figs. 5c and 6c). The amount of Mc present decreases between 7 and 90 days, while quantities of both C_3AH_6 and AH_3 increase during the same period. This destabilization of Mc with respect to C_3AH_6 is not expected—as Mc is anticipated to remain stable (at ambient temperature) with respect to C_3AH_6 and the calcium salt, whose anion is contained in the AFm interlayer position. In contrast, in CAC–limestone blends, at high w/s (e.g., for $w/s = 0.70$), the amount of C_3AH_6 present is negligible as compared to the Mc content (Fig. 3c).

The destabilization of Mc to C_3AH_6 over the course of time in the Na_2CO_3-rich systems is speculated to be on account of differences in the binder chemistry. These differences in Na_2CO_3 mixtures as compared to $CaCO_3$ systems are likely due to changes in the $CO_{2\text{-eq}}/CaO$ ratio (Fig. 1c) with increasing CAC replacement. This implies that systems with a higher $CO_{2\text{-eq}}/CaO$ ratio form phases with a higher CO_3^{2-} and a lower Ca^{2+} content (i.e., as compared to Mc and Hc), which in an Na^+-concentrated environment results in the formation of gaylussite or thermonatrite. The formation of gaylussite and thermonatrite consumes a large quantity of water (e.g., 5 and 1 molar units of water, respectively, are taken up per formula unit of gaylussite and thermonatrite), which may lead to the formation of C_3AH_6 as the dominant stable phase due to its low water content, and simultaneously prevent carboaluminate phase formation. A similar hindrance in NO_3-AFm phase formation due to limited water availability was also noted when $Ca(NO_3)_2$ was used as an agent to suppress conversion in CACs [13] (i.e., to form the favored NO_3-AFm phase) suggesting that bulk chemical composition is an insufficient indicator of the ability to prevent conversion—but rather, the amount of water present is also a relevant variable.

Unlike $CaCO_3$-containing systems, blends containing lower Na_2CO_3 contents (10 mass%) show the formation of Hc at early ages (see Fig. 5a, b). The Hc formed converts to Mc at later ages. While such
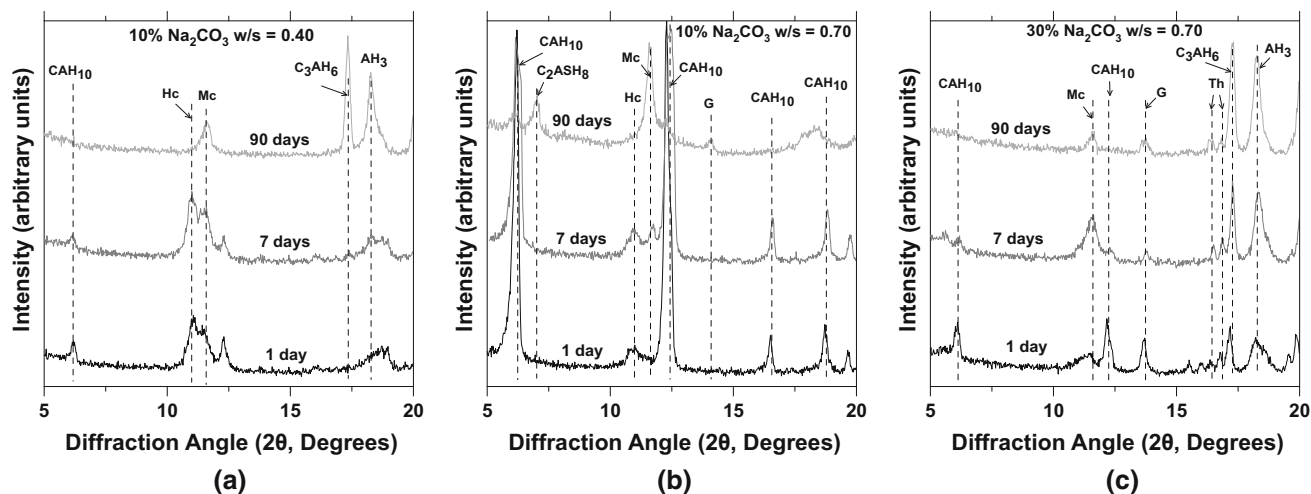
Figure 5 Representative XRD patterns of the hydrated CAC–Na$_2$CO$_3$ blends for **a** $w/s = 0.40$, 10 % Na$_2$CO$_3$, **b** $w/s = 0.70$, 10 % Na$_2$CO$_3$, and **c** $w/s = 0.70$, 30 % Na$_2$CO$_3$. In all plots, *G* gaylussite (Na$_2$Ca(CO$_3$)$_2$·5H$_2$O), *Th* thermonatrite (Na$_2$CO$_3$·H$_2$O), *Mc* monocarboaluminate (Ca$_4$Al$_2$(CO$_3$)(OH)$_{12}$·5H$_2$O), and *Hc* hemicarboaluminate (Ca$_4$Al$_2$(CO$_3$)$_{0.5}$(OH)$_{13}$·5.5H$_2$O).
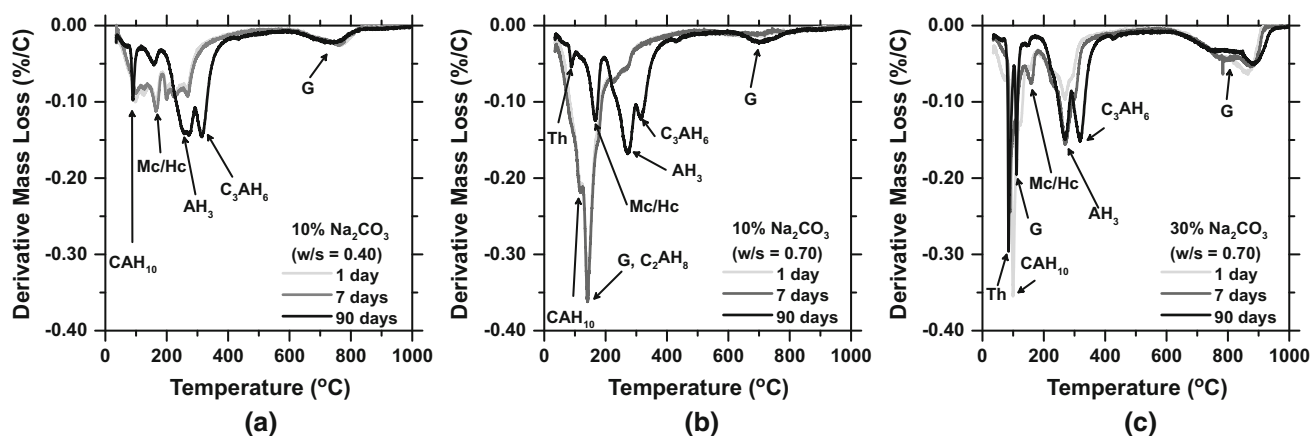

Figure 6 Representative DTG traces for the hydrated CAC–Na$_2$CO$_3$ blends for **a** $w/s = 0.40$, 10 % Na$_2$CO$_3$, **b** $w/s = 0.70$, 10 % Na$_2$CO$_3$, and **c** $w/s = 0.70$, 30 % Na$_2$CO$_3$. In all plots, *G* gaylussite (Na$_2$Ca(CO$_3$)$_2$·5H$_2$O), *Th* thermonatrite (Na$_2$CO$_3$·H$_2$O), *Mc* monocarboaluminate (Ca$_4$Al$_2$(CO$_3$)(OH)$_{12}$·5H$_2$O), and *Hc* hemicarboaluminate (Ca$_4$Al$_2$(CO$_3$)$_{0.5}$(OH)$_{13}$·5.5H$_2$O).

behavior is seen in OPC systems containing limestone where the formation of Hc precedes Mc [44], this behavior is not observed in CAC blends with limestone (see Fig. 3) where Mc forms rapidly. Taken together, these results note the relevance of (i) water availability, (ii) solubility of the carbonate source, and (iii) calcium content of the carbonate source as major variables which influence stable phase relations in CAC blends that are hydrated at 25 °C and under sealed conditions.

Thermodynamic calculations

Role of water content on phase equilibria

A series of thermodynamic calculations were carried out to understand, parametrically, how the water content of a given mixture influences stable phase equilibria when CAC is replaced by a carbonate source. Figure 7 shows equilibrium phase assemblages assessed in blends wherein 10 mass% of the
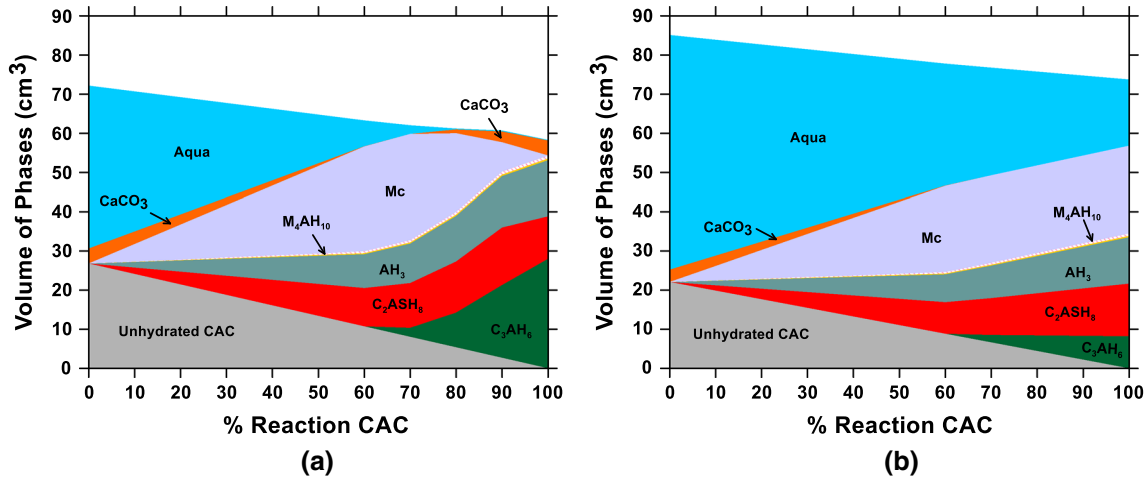
Figure 7 Volumetric phase assemblage calculated to exist when 10 mass% CAC has been replaced by limestone ($CaCO_3$) for **a** $w/s = 0.40$ and **b** $w/s = 0.70$. In these plots, Mc monocarboaluminate ($Ca_4Al_2(CO_3)(OH)_{12} \cdot 5H_2O$) and M_4AH_{10} OH-hydrotalcite.

CAC has been replaced by limestone. In general, systems prepared at lower w/s (e.g., $w/s = 0.40$) show the increasing formation of Mc and AH_3, until water is exhausted (Fig. 7a). The formation of C_3AH_6 is prevented so long as free water is available. However, once free water is consumed (around 70 % CAC reaction), Mc decomposes or stops forming, and other phases such as AH_3, C_3AH_6, and $CaCO_3$ are expected to precipitate. Such sacrificial behavior of Mc, in favor of C_3AH_6 and $CaCO_3$, in water-deficient systems is not observed experimentally as Mc continues to form over time (i.e., as the CAC reaction progresses) despite the low water content (see Fig. 3a)—at least until 90 days. This points to the stability of Mc in CAC–limestone systems, wherein once formed, this phase remains stable in spite of low water availability. It is however possible that the decomposition of Mc into $CaCO_3$ and C_3AH_6 occurs at times later than 90 days.

In cases where water is abundant, Mc persists as long as limestone is present (see Fig. 7b). But, when limestone is consumed, expectedly, C_3AH_6 forms as a stable phase. In agreement with experimental data (Fig. 3), the calculations predict the formation of C_2ASH_8 (strätlingite) due to the C_2AS hydration, in water-deficient and water-rich systems (Fig. 7). The calculations also suggest that under water-rich and kinetically unconstrained conditions, as long as limestone is present, the conversion process can be mitigated. This is however unrealistic because under practical conditions the ability to suppress conversion when limestone is present is negligible [24]. This

discrepancy arises because the calculations due to their equilibrium nature do not account for the slow dissolution of $CaCO_3$—which prevents it from serving as an effective conversion suppression agent. As a result, at any extent of CAC reaction, the calculations overestimate the amount of $CaCO_3$ consumed, the quantity of Mc formed, and thus the success (or lack thereof) of mitigating the conversion phenomena.

Figure 8 shows equilibrium phase assemblages in water-rich ($w/s = 0.70$) systems where 10 and 30 mass% CAC have been replaced by Na_2CO_3. In these cases, the formation of C_3AH_6 is either delayed or negated with rising Na_2CO_3 dosages and with an increasing extent of CAC reaction. At modest Na_2CO_3 dosages (10 mass%), AH_3 and Mc are predicted to form (Fig. 8a), the latter by the uptake of CO_3^{2-} species solubilized in the pore fluid, while Na^+ remains mobile in the pore solution (N.B.: alkali uptake is not considered herein). When Na_2CO_3 dosages are increased, gaylussite ($Na_2Ca(CO_3)_2 \cdot 5H_2O$) forms with a corresponding decrease in the amount of AH_3 and Mc present—in agreement with XRD and DTG data as shown in Figs. 5c and 6c, respectively. The formation of gaylussite is ensured by the need to allocate sodium and carbonate species, which in turn penalizes the formation of Mc (see Fig. 8b).

The formation of water-rich phases (gaylussite and thermonatrite), and their resultant water uptake, does not trigger the formation of C_3AH_6 (a dense, low-water content phase) as seen in the XRD data (a Fig. 5c) and Mc continues to form unimpeded
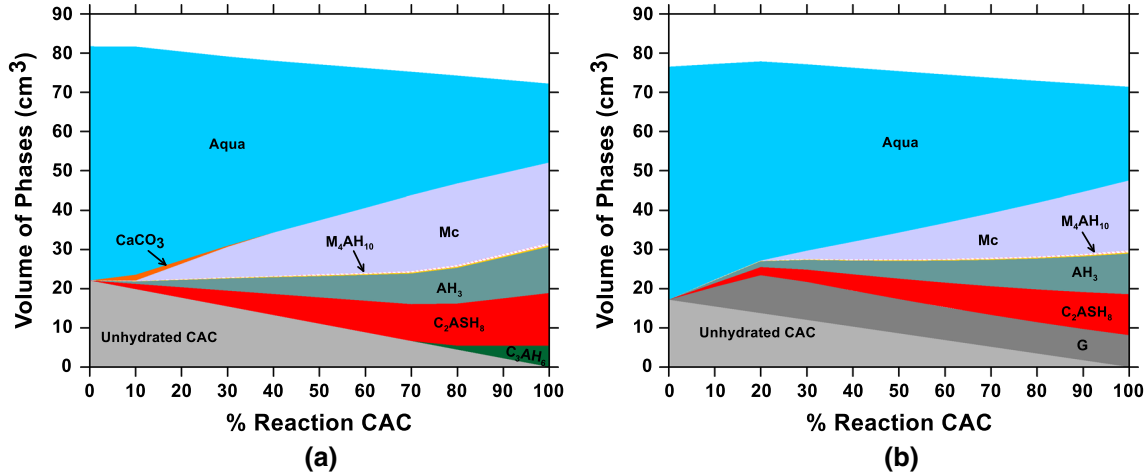
Figure 8 Volumetric phase assemblage calculated to exist for $w/s = 0.70$ when CAC has been replaced by Na_2CO_3 at the level of (by mass) **a** 10 mass% and **b** 30 mass%. In these plots, G gaylussite ($Na_2Ca(CO_3)_2 \cdot 5H_2O$), Mc monocarboaluminate ($Ca_4Al_2(CO_3)(OH)_{12} \cdot 5H_2O$), and M_4AH_{10} OH-hydrotalcite.

(Fig. 8). While the reasons for this discrepancy are not fully clear, it is thought to be on account of the calculations being unable to account for the water activity-dependent stability of Mc, which destabilizes below a critical water activity [45, 46], or due to C_3AH_6 formation in inhomogeneous microstructural zones. Water activity is discussed, as the solubilization of Na_2CO_3 into the mixing water would result in significant reductions in the water activity. It is seen that thermonatrite (Th, $Na_2CO_3 \cdot H_2O$), although present in the XRD data (Fig. 5c), is absent in the predicted phase assemblages at equilibrium (Fig. 8b). This is thought to be because thermonatrite forms at the time of early CAC hydration, i.e., when Na_2CO_3 is added to the mixing water and remains unaffected thereafter (e.g., see near-constant thermonatrite intensities in the XRD patterns across all ages).

Role of the calcium content of the carbonate source

To estimate the effects of the "calcium content" of the carbonate source, a new series of simulations were carried out. Here, the level of CAC replacement (by a carbonate source) varies between 0 and 50 mass%. At each replacement increment, a process simulation was carried out, in which the amount of carbonate source was progressively reduced while increasing the CaO content of the system, i.e., to simulate the influence of CaO that could accompany the carbonate salt. In these calculations, the quantity of the carbonate source and additional CaO provided (i.e., over and above CaO contributed by the CAC) was fixed according to the level of CAC replacement. For example, in the case of a 30 mass% CAC replacement, the CaO-to-carbonate source ratio (see x-axis in Fig. 9) ranges from 0.93 to 18.30 for both carbonate sources (Na_2CO_3 and $CaCO_3$).

Figure 9 shows the volumetric phase assemblage as a function of an increase in the CaO-to-carbonate source ratio. It is seen that the phase assemblage alters significantly as CaO/XCO_3 ratio (where $X = Ca, Na$) increases. Specifically, the amount of Mc produced, by both carbonate sources, initially increases and then reaches a maximum at a $CaO/XCO_3 \approx 2.0$ and decreases thereafter. $CaCO_3$ is slightly more efficient than Na_2CO_3 in forming Mc at a similar CaO/XCO_3 value on account of (a) its greater provision of Ca^{2+} ions when $X = Ca$ than $X = Na$, and (b) limestone's low solubility which implies that water activity of the pore fluid is higher when $X = Ca$ than $X = Na$, a condition that potentially favors the formation of Mc. This points to the relevance of the carbonate source's calcium content and its solubility as factors controlling carboaluminate phase formation in CAC systems.

Summary and conclusions

The influences of slightly ($CaCO_3$) and highly soluble (Na_2CO_3) carbonate salts on hydrated phase relations in calcium aluminate cements (CACs) have been critically examined. It has been shown that water
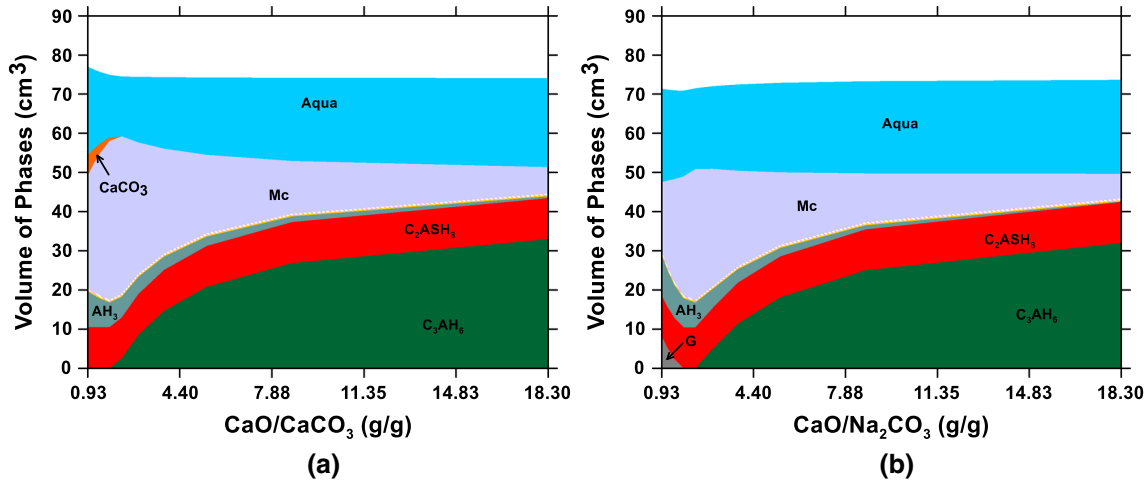
Figure 9 Volumetric phase assemblage calculated to exist for $w/s = 0.70$ when 30 mass% of the CAC has been replaced by a combination of **a** CaO and $CaCO_3$ and **b** CaO and Na_2CO_3. In these plots, *G* gaylussite ($Na_2Ca(CO_3)_2 \cdot 5H_2O$), *Mc* monocarboaluminate ($Ca_4Al_2(CO_3)(OH)_{12} \cdot 5H_2O$), and M_4AH_{10} OH-hydrotalcite.

availability and the solubility and calcium content of the carbonate source play important and interrelated roles in the formation of carboaluminate phases. In the case of slightly soluble carbonates ($CaCO_3$), a higher water availability (and water activity) is linked to an increase in carbonate source consumption and carboaluminate (Mc) phase formation. These conclusions are supported by experimental observations of thermogravimetric and X-ray diffraction datasets. Comparisons between thermodynamic calculations and experimental results reveal that $CaCO_3$ consumption is limited due to the low aqueous solubility and dissolution rate of $CaCO_3$—which are the limiting factors in carboaluminate phase formation.

To overcome the limitations of $CaCO_3$ use, a soluble carbonate salt (Na_2CO_3) was studied as a potentially more reactive carbonate source. Despite its high solubility, thermogravimetric and X-ray diffraction data show that Na_2CO_3 also fails to boost carboaluminate phase formation. In this case, the formation of other carbonate-bearing phases (i.e., gaylussite and thermonatrite) that compete for CO_3^{2-} ions suppress carboaluminate phase formation. The formation of these other carbonate phases (i.e., which lack aluminum and feature a lower Ca^{2+} content as compared to the carboaluminate hydrates), and the persistence of AH_3 in Na_2CO_3 systems, indicates that the calcium content of the carbonate source is a key variable which influences carboaluminate phase formation. It is noted that reductions in water activity resulting from the solubilization of ions negatively affect carboaluminate phase formation. It is thus concluded that, independent of the carbonate salt used, carboaluminate phase formation is not a viable solution to mitigate conversion phenomena in hydrated CACs.

Acknowledgements

References

[1] De Weerdt K, Ben Haha M, Le Saout G et al (2011) Hydration mechanisms of ternary Portland cements containing limestone powder and fly ash. Cem Concr Res 41(3):279–291

[2] Damidot D, Glasser FP (1995) Thermodynamic investigation of the CaO—Al$_2$O$_3$—CaSO$_4$—CaCO$_3$-H$_2$O closed system at 25 °C and the influence of Na2O. Adv Cem Res 7(27):129–134

[3] Damidot D, Lothenbach B, Herfort D, Glasser FP (2011) Thermodynamics and cement science. Cem Concr Res 41(7):679–695

[4] Kumar A, Oey T, Kim S, Thomas D, Badran S, Li J, Fernandes F, Neithalath N, Sant G (2013) Simple methods to estimate the influence of limestone fillers on reaction and property evolution in cementitious materials. Cem Concr Compos 42:20–29

[5] Lothenbach B, Winnefeld F (2006) Thermodynamic modelling of the hydration of Portland cement. Cem Concr Res 36(2):209–226

[6] Lothenbach B, Le Saout G, Gallucci E, Scrivener K (2008) Influence of limestone on the hydration of Portland cements. Cem Concr Res 38(6):848–860

[7] Matschei T (2007) Thermodynamics of cement hydration PhD diss., Aberdeen University, Aberdeen

[8] Matschei T, Lothenbach B, Glasser FP (2007) The AFm phase in Portland cement. Cem Concr Res 37(2):118–130

[9] Oey T, Kumar A, Bullard JW, Neithalath N, Sant G (2013) The filler effect: the influence of filler content and surface area on cementitious reaction rates. J Am Ceram Soc 96(6):1978–1990

[10] Tomaž V, Tinta V, Gabrovšek, Kaučič V (2001) The effects of limestone addition, clinker type and fineness on properties of Portland cement. Cem Concr Res 31(1):135–139

[11] Tsivilis S, Chaniotakis E, Kakali G, Batis G (2002) An analysis of the properties of Portland limestone cements and concrete. Cem Concr Compos 24(3):371–378

[12] Puerta-Falla G, Balonis M, Le Saout G, Falzone G, Zhang C, Neithalath N, Sant G (2015) Elucidating the role of the aluminous source on limestone reactivity in cementitious materials. J Am Ceram Soc 98(12):4076–4089

[13] Falzone G, Balonis M, Sant G (2015) X-AFm stabilization as a mechanism of bypassing conversion phenomena in calcium aluminate cements. Cem Concr Res 72:54–68

[14] Lothenbach B, Pelletier-Chaignat L, Winnefeld F (2012) Stability in the system CaO–Al$_2$O$_3$–H$_2$O. Cem Concr Res 42(12):1621–1634

[15] Scrivener KL, Capmas A (1998) Lea's Chemistry of cement and concrete calcium aluminate cements, Chapter 13, In: Hewlett PC (ed), Wiley, New York

[16] Scrivener KL, Cabiron JL, Letourneux R (1999) High-performance concretes from calcium aluminate cements. Cem Concr Res 29(8):1215–1223

[17] Puerta-Falla G, Kumar A, Gomez-Zamorano L, Bauchy M, Neithalath N, Sant G (2015) The influence of filler type and surface area on the hydration rates of calcium aluminate cement. Constr Build Mater 96:657–665

[18] Klaus SR, Neubauer J, Goetz-Neunhoeffer F (2013) Hydration kinetics of CA$_2$ and CA—investigations performed on a synthetic calcium aluminate cement. Cem Concr Res 43:62–69

[19] Taylor HFW (1997) Cement Chemistry, 2nd edn. Thomas Telford, London

[20] Mangabhai RJ, Glasser FP (2001) Calcium Aluminate Cements. IOM communications, London

[21] Shahwana R, Barnes P, Bensted J, Turrillas X (1994) Conversion of calcium aluminate cement hydrates re-examined with synchrotron energy-dispersive diffraction J Mater Sci lett 13(17):1232–1234

[22] Ukrainczyk N, Šipušić J, Dabić P, Matusinović T (2008) Microcalorimetric study on calcium aluminate cement hydration. 13th International conference on materials, processes, friction and wear, p 382–388

[23] Kuzel HJ (1996) Initial hydration reactions and mechanisms of delayed ettringite formation in Portland cements. Cem Concr Compos 18(3):195–203

[24] Luz AP, Pandolfelli VC (2012) CaCO$_3$ addition effect on the hydration and mechanical strength evolution of calcium aluminate cement for endodontic applications. Ceram Int 38(2):1417–1425

[25] ASTM (International and American Society for Testing & Materials) (2004) Annual book of ASTM standards, American Society for Testing & Materials, USA

[26] National Center for Biotechnology Information (NCBI)—PubChem database. Available at https://www.ncbi.nlm.nih.gov/pccompound. Accessed 10 Dec 2015

[27] FIZ/NIST—Inorganic crystal structure database (ICSD) (version 2009/1). Available for purchase at http://www.nist.gov/srd/nist84.cfm

[28] Mineralogical Society of America—American mineralogist crystal structure database. Available at http://rruff.geo.arizona.edu/AMS/amcsd.php. Accessed 15 Jan 2015

[29] Le Saout G, Kocaba V, Scrivener KL (2011) Application of the Rietveld method to the analysis of anhydrous cement. Cem Concr Res 41:133–148

[30] Kulik D (2013) GEMS-PSI 2.1. Available at http://les.web.psi.ch/Software/GEMS-PSI/. Accessed 18 June 2013

[31] Myers RJ, Lothenbach B, Bernal SA, Provis JL (2015) Thermodynamic modelling of alkali-activated slag cements. Appl Geochem 61:233–247

[32] Martin LHJ, Winnefeld F, Müller CJ, Lothenbach B (2015) Contribution of limestone to the hydration of calcium sulfoaluminate cement. Cem Concr Compos 62:204–211

[33] Thomas JJ, Jennings HM (1998) Free-energy-based model of chemical equilibria in the CaO–SiO$_2$-H$_2$O system. J Am Ceram Soc 81(3):606–612

[34] Paul Scherrer Institute—GEMS: Gibbs free energy software for geochemical modeling. Available at http://gems.web.psi.ch/. Accessed 18 June 2015

[35] Lothenbach B—CEMDATA. Available at http://www.empa.ch/web/s308/cemdata. Accessed 18 June 2014

[36] Haha MB, Lothenbach B, Le Saout G, Winnefeld F (2012) Influence of slag chemistry on the hydration of alkali-activated blast-furnace slag—Part II: effect of Al_2O_3. Cem Concr Res 42(1):74–83

[37] Pelletier-Chaignat L, Winnefeld F, Lothenbach B, Müller CJ (2012) Beneficial use of limestone filler with calcium sulphoaluminate cement . Constr Build Mater 26(1):619–627

[38] Geoscience for a sustainable earth—Mineral species data base. Available at http://thermoddem.brgm.fr/data/mineraux.php. Accessed on 15 Jan 2015

[39] Önder K, Yaman IO, Tokyay M (2013) Compressive strength development of calcium aluminate cement–GGBFS blends. Cem Concr Compos 35(1):163–170

[40] Lothenbach B, Le Saout G, Gallucci E, Scrivener K (2008) Influence of limestone on the hydration of Portland cements. Cem Concr Res 38(6):848–860

[41] Johnson DR, Robb WA (1973) Gaylussite: thermal properties by simultaneous thermal analysis. Am Mineral 58:778–784

[42] Hartmant M, Trnka O, Vesely V, Karel Svodoba (2001) Thermal dehydration of the sodium carbonate hydrates. Chem Eng Commun 185(1):1–16

[43] Steudel A, Mehl D, Emmerich K (2013) Simultaneous thermal analysis of different bentonite–sodium carbonate systems: an attempt to distinguish alkali-activated bentonites from raw materials. Clay Miner 48(1):117–128

[44] Matschei T, Lothenbach B, Glasser FP (2007) The role of calcium carbonate in cement hydration. Cem Concr Res 37(4):551–558

[45] Baquerizo LG, Matschei T, Scrivener KL, Saeidpour M, Wadsö L (2015) Hydration states of AFm cement phases. Cem Concr Res 73:143–157

[46] Baquerizo LG (2015) Impact of water activity on the mineralogy of hydrated cement Ph.D. diss. École Polytechnique Fédérale de Lausanne, Lausanne